Two-dimensional aggregation of polystyrene latex particles

Jolanta Stankiewicz
Departamento de Física Aplicada, Universidad de Granada, 18071 Granada, Spain
and Centro de Física, Instituto Venezolano de Investigaciones Científicas, Apartado 21827, Caracas 1020A, Venezuela

Miguel A. Cabrerizo Vílchez and Roque Hidalgo Alvarez
Departamento de Física Aplicada, Universidad de Granada, 18071 Granada, Spain
(Received 3 August 1992)

Salt-induced aggregation of polystyrene latex confined to two dimensions on an air-water interface has been studied. Fractal dimensions of the aggregates are determined (i) from relation between the radius of gyration and cluster masses and (ii) by the box method. They both increase with aggregation time. While the fractal dimensions are insensitive to electrolyte concentration, the aggregation rate does depend on it. Our results for aggregation kinetics are in good agreement with the dynamic scaling law $n_m(t) \sim m^{-2} f(m/t^z)$, for $z=1$, for dilute latex dispersions [$n_m(t)$ is the number of clusters of size m at time t]. A nonlinear behavior in time, however, is observed for more concentrated latex dispersions. We find bell-shaped cluster-size distributions.

PACS number(s): 82.70.Dd

I. INTRODUCTION

Aggregation in colloidal suspensions has been the subject of many theoretical, computer-simulation, and experimental studies recently [1–7]. It is an important phenomenon in a wide variety of physical [1], chemical [8], and biological [9] processes. Colloid aggregates are highly ramified fractal structures [10]. It is now generally accepted that there exist two limiting regimes of irreversible colloid aggregation: fast diffusion-limited cluster aggregation (DLCA) and slow reaction-limited cluster aggregation (RLCA) [11]. Fractal dimensions, cluster-size distribution, and aggregation kinetics are specific to each regime. The two limiting behaviors are believed to be universal in the sense that they do not depend on details of interparticle interactions. Indeed, it has been shown recently that various systems such as colloidal gold, silica, and polystyrene do exhibit such universal behavior [4,5].

In the DLCA regime aggregation is limited only by diffusion of colloid particles. The fractal dimension D of grown structures is about 1.45 in two dimensions ($d=2$) and about 1.80 in $d=3$. Average cluster mass grows linearly with the time of aggregation. In the RLCA regime repulsive forces between particles are not negligible and their Brownian motion is therefore not independent. This leads to much slower rates of aggregation and to the formation of more compact structures. RLCA clusters grow exponentially in time; furthermore $D \cong 1.6$ and 2.10 in $d=2$ and 3, respectively. Most aggregation experiments do not meet conditions for ideal DLCA or RLCA processes. Consequently, both fractal morphology and aggregation kinetics may deviate from the predicted ones. Some experimental results can be interpreted as a crossover behavior in the intermediate regime between RLCA and DLCA, although deviations are too large and unexplained sometimes [12,13].

By now, the number of theoretical predictions and computer simulations exceed the number of experimental results by far. In two-dimensional systems, fractal dimensions ranging from 1.2 to 1.74 have been obtained under different experimental conditions [14–16]. In particular, the result of Hurd and Schaefer [16] of $D=1.20\pm0.15$, found for aggregation of silica particles on an air-water interface, has motivated calculations in which long-range interactions between aggregating particles have been invoked [17]. Other models [18,19] that take into account effects of cluster-cluster interactions also yield smaller values for D in $d=2$. However, there is no clear theoretical picture of two-dimensional aggregation thus far.

In this paper, we report results of a two-dimensional aggregation experiment. We have studied salt-induced aggregation of polystyrene particles confined to an air-water interface using direct visual observation with a phase-contrast microscope and computer image-analysis methods. The fractal dimension, cluster-size distribution, and time evolution of average cluster masses have been determined for various electrolyte concentrations and two different, polystyrene monomer concentrations. We have found that the fractal dimension D_1, obtained from the relation between the radius of gyration and mass of clusters, is about 1.48 for large mean cluster masses, for all electrolyte concentrations studied. This value is close to the one found in DLCA two-dimensional simulations ($D \cong 1.45$) [7]. However, we believe that the asymptotic value of D_1 may be larger since it shows a tendency to increase with increasing aggregation time. On the other hand, the Hausdorff-Besicovitch fractal dimensionality, D_2, of largest clusters observed at various stages of aggregation varies significantly with cluster mass m: from a value of about 1.1, for small clusters ($m \cong 10^2$), to a value of about 1.6 for large aggregates ($m \cong 3\times10^4$). This behavior has been found for all salt concentrations used. For more dilute polystyrene concentrations, the mean cluster mass grows about linearly with the aggregation

time. The dynamic scaling law $n_m(t) \sim m^{-2} f(m/t^z)$, where $n_m(t)$ is the number of clusters of size m at time t, is obeyed for $z=1$, in agreement with the DLCA model predictions. A nonlinear behavior in time is observed for more concentrated latex dispersions. Bell-shaped cluster-size distributions are found in all runs.

The outline of this paper is as follows: in Sec. II we describe experimental details; results are reported and discussed in Sec. III; the conclusions are in Sec. IV.

II. EXPERIMENT

A monodisperse sulfonated polystyrene colloid was used in this study. The polystyrene spheres had a diameter of 178 ± 8 nm and their surface-charge density was $-(17\ \mu C/cm^2)$ [20]. All polystyrene latex suspensions were first carefully cleaned by ultrafiltration. The samples were prepared by spreading techniques [16,21]. A small amount of freshly cleaned latex, dispersed in 20% aqueous methanol, was carefully added from a microsyringe to the flat surface of the electrolyte solution. We used two monomer concentrations corresponding roughly to 1×10^7 and 5×10^7 particles/cm^2. They were spread over an area of about 0.25 cm^2. Aggregation was induced by adding sodium chloride (NaCl) to the solution. The effect of salt ions is to decrease the Debye-Hückel screening length, and thus to lower the repulsive barrier between charged latex particles [22]. The electrolyte concentrations used varied from $0.2M$ to $1.0M$ in order to cover diverse regimes of aggregation. To assure DLCA conditions, hydrochloric acid (HCl) was added to a concentration of $1.5M$ in two runs. In this regime, the time required for the polystyrene clusters to reach a size of 40 μm was about 30 min; that is about ten times less than the time needed for clusters to reach the same size in a $0.25M$ NaCl solution.

After spreading of latex five to ten minutes were allowed for solvent evaporation before measurements. Optical observations and photographs were made during each aggregation experiment using a phase-contrast microscope. A magnification of $400\times$ was used throughout with a corresponding resolution of about 0.8 μm. We observed single particles sticking to each other initially and cluster-cluster aggregation at later times. The micrographs obtained (Fig. 1) were digitized and further analysis was done on a computer workstation. Since individual particles within a cluster could not be resolved in the photographs, equal-mass segments were judged by eye (about five particles per segment). This can introduce systematic errors; however, it does not affect the scaling relations used to determine the fractal dimension. In addition, several photographs were analyzed by a digital image processor. We did not find any change in results despite the fact that the assignment of the equal-mass segments was somewhat arbitrary.

Only solvents of spectroscopic grade were used. All electrolyte solutions were prepared with Millipore Milli-Q filtered water (with a resistivity of about 18 MΩ cm) and all experiments were performed at a temperature of (20 ± 1) °C.

III. RESULTS AND DISCUSSION

A. Fractal structure

We used two methods to measure the fractal dimension of the aggregates. First, we determined the radius of gyration of clusters, R_g, as a function of the cluster mass m (which is proportional but not equal to the number of particles) at various stages of aggregation. A plot of the logarithm of R_g versus the logarithm of m is shown in Fig. 2 for 157 clusters observed in one of the experimental runs. Linear dependence holds over more than two decades in mass. The inverse of the slope gives the frac-

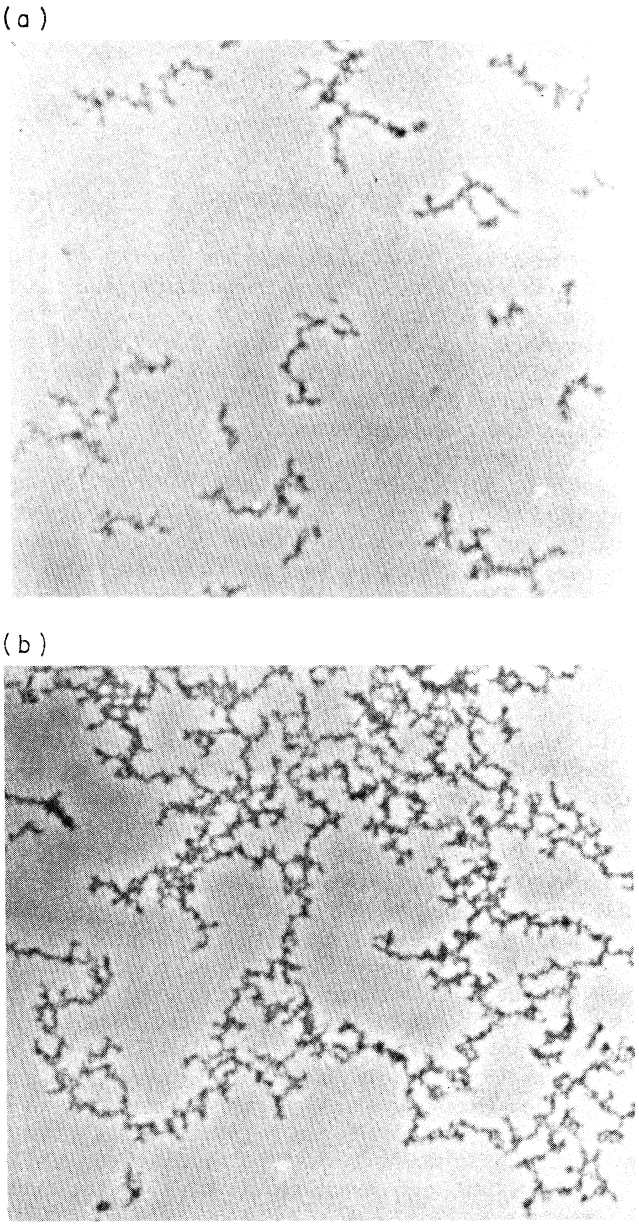

FIG. 1. Photograph of clusters obtained for $1.5M$ NaCl at two aggregation stages: (a) 10 min and (b) 270 min after dispersion. Area shown is about $150 \times 150\ \mu m^2$.

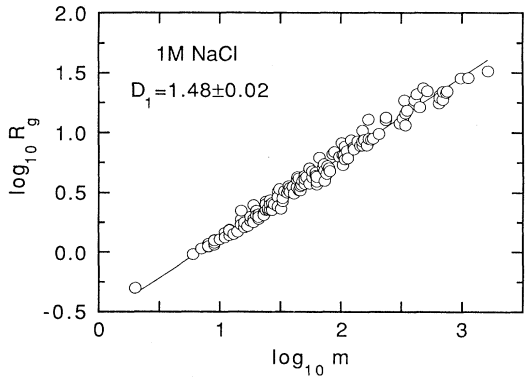

FIG. 2. A plot of the logarithm of the radius of gyration R_g vs the logarithm of cluster mass m (m is the number of equal-mass segments counted in the cluster). The inverse of the slope gives the fractal dimension D_1.

tal dimension D_1, as $R_g \sim m^{1/D_1}$. Second, we used the box method to find the Hausdorff-Besicovitch [23] fractal dimension D_2 of the largest clusters observed at different aggregation times. In this method, the number of square and nonoverlapping boxes $N(\epsilon)$ of side ϵ needed to cover a cluster is determined; it scales like $N(\epsilon) \sim \epsilon^{-D_2}$.

Figure 3 shows the fractal dimension D_1 for various salt concentrations as a function of the mean cluster size (mass) $S(t)$ defined by [2]

$$S(t) = \sum_m m^2 n_m(t) / \sum_m m n_m(t) , \quad (1)$$

where $n_m(t)$ is the total number of clusters of mass m at time t. The data shown correspond to different stages of aggregation between 10 min and 3 h. We could not determine D_1 for longer times because of limitations in our experimental setup. The scatter in the values of D_1 is large; nevertheless a trend of an increase with increasing $S(t)$ (or t) is observed. This trend is more obvious for lower electrolyte concentrations. For large mean cluster masses, $D_1 \cong 1.48$. This is close to the value found in two-dimensional DLCA simulations ($D \cong 1.45$) [7].

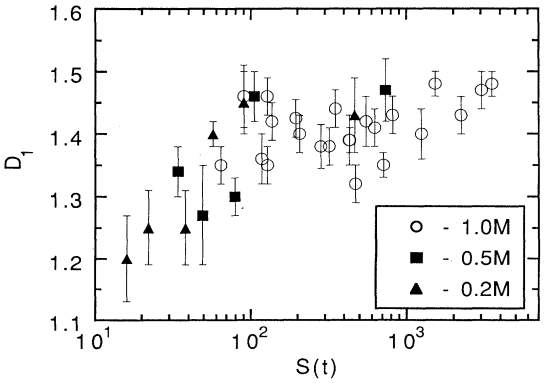

FIG. 3. Variation of the fractal dimension D_1 (obtained from the relation between the radius of gyration and cluster mass) with mean cluster size $S(t)$ for three different electrolyte concentrations.

However, we believe that D_1 is larger for larger values of $S(t)$, which we could not observe. A value of $D_1 \cong 1.55 \pm 0.03$ was obtained, after 30 min, for a fast aggregation run (when HCl was added to the electrolyte solution).

Figure 4 shows values of D_2 found for the largest clusters within the field of view formed at various stages of aggregation. D_2 varies significantly with cluster mass m: from a value of about 1.1 for the smallest clusters to a value of about 1.6 for the largest aggregates observed. This behavior for over two decades in mass was found for all electrolyte concentrations used in our experiments. For the largest clusters which we could measure, $m \cong 3 \times 10^4$, D_2 is about 1.6, in agreement with the value obtained in two-dimensional RLCA simulations [6]. The data points shown in Fig. 4 seem to follow the simple relation $D_2 \sim m^{\alpha}$, with $\alpha = 0.06$, in the $10^2 \leq m \leq 3 \times 10^4$ range. This fit is clearly not to be extrapolated too far as it leads to $D_2 > 2$. Other relations, for instance, $D_2 = 1.6 - \exp(-\beta m)/m^{\gamma}$, with $\beta \cong 10^{-4}$ and $\gamma \cong 0.16$, also fit the data (as shown by a dashed line in Fig. 4) just as well. The latter relation saturates at a value of 1.6 as $m \to \infty$. Clearly, we cannot discriminate between these fits.

Whereas (surprisingly), the fractal structures studied are insensitive to electrolyte concentration, the aggregation rates do depend on it. That is discussed in the next subsection. Both fractal dimensions, D_1 and D_2, become larger as the aggregation proceeds; D_2 seems (perhaps) to tend to a limiting value of about 1.6. In our experiment, latex particles are assumed to be trapped by surface-tension forces at the air-water interface. The surface-energy well is deep enough [24] to assure that the system studied is strictly two dimensional. Furthermore, the effect of gravitational forces is negligible [24]. Thus particles float on a completely flat interface. Taking into account only electrostatic interactions, we would expect a variation in the fractal dimension of aggregates formed at different electrolyte concentrations. With increasing salt concentration, electrostatic repulsion between latex particles should decrease while the van der Waals attraction remains essentially unchanged. Consequently, as electro-

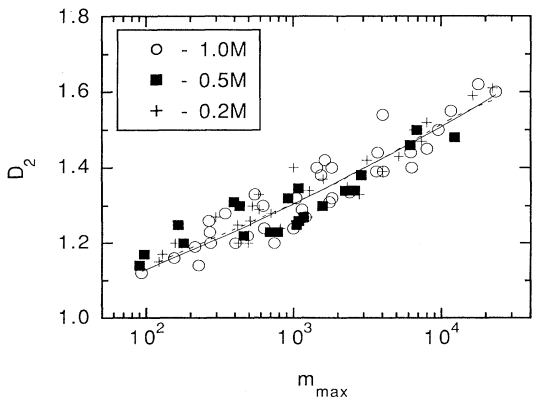

FIG. 4. Variation of the Hausdorff-Besicovitch fractal dimension D_2 with cluster mass for three different electrolyte concentrations.

lyte concentrations increase, the aggregation process should cross over from RLCA- to DLCA-like behavior, with the fractal dimension crossover between the two corresponding limiting values. No such variation takes place, however. That suggests that other effects are more important. In particular, anisotropic repulsive interactions may account for the low dimensionality of clusters at early stages of aggregation. Hurd and Schaefer argued that a barrier for a particle approaching a dimer is orders of magnitude lower for end-on approach than for side-on approach [16]. That would lead to less branching and lower D. In addition, simulations by Jullien [18,19] have shown that D is reduced when cluster polarization effects favoring sticking on tips are taken into account. In our system, these interactions are expected to be independent of salt concentration.

The fact that D grows with time suggests the idea of "restructuring" that is related to not-fully-irreversible bond formation [25,26]. In many cases aggregation may be thought of as a process of several stages. First, clusters stick to each other and are held together by van der Waals attractive forces. Thermal or external force fluctuations can, however, disrupt these relatively weak interactions and produce rearrangement of particles leading to more compact structures. Indeed, numerical simulations of a cluster-cluster reversible aggregation model show that restructuring can give rise to an appreciable increment of the fractal dimension with time [26]. It has been found experimentally that rapid aggregation produces clusters with an initially lower fractal dimension ($D \cong 1.75$ in $d=3$) which restructure within a period of hours (days) to more compact stable aggregates with $D \cong 2.1(2.4)$ [25,27]. However, no spontaneous restructuring was observed in a recent detailed study [28]. Thus, although restructuring seems to offer a reasonable explanation for the observed variation of D with m, it remains to be established whether restructuring is an intrinsic effect or is produced by some external perturbation. We find it interesting that restructuring yields aggregates that have about the same fractal dimension as RLCA grown clusters. To our knowledge, restructuring effects had not been observed in two-dimensional systems to date.

B. Aggregation kinetics

The total number of clusters in the system, $N(t)=\sum_m n_m(t)$, normalized to a unit surface, and the mean cluster size $S(t)$ were determined at various stages of the aggregation experiment. In some cases, the data for a small range of cluster sizes were averaged to obtain the final results. Figure 5 shows how $S(t)$ varies with time for a dilute latex dispersion at three different electrolyte concentrations. A linear behavior $S(t) \sim t$ holds over a decade and a half in time. Aggregation proceeds faster for more concentrated electrolytes; the growth rate of aggregates for $0.25M$ solution is more than an order of magnitude lower than the growth rate for $1.5M$ solution (quite likely in the DLCA limit). Figure 6 shows how $S(t)$ and $N(t)$ vary with time for $1M$ NaCl solution. It is observed that $S(t) \sim t^z$ and $N(t) \sim t^{-z}$, with $z = 1.1 \pm 0.1$.

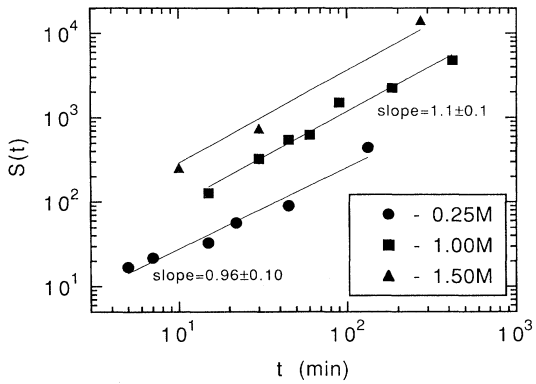

FIG. 5. Mean aggregate size $S(t)$ as a function of aggregation time for a dilute latex dispersion on three different electrolyte solutions.

Such behavior is a consequence of dynamic-scaling theory [2,29]. It has been shown that Monte Carlo results [2,30–32] can be well described by a scaling function of the form

$$n_m(t) \sim m^{-2} f(m/t^z) , \tag{2}$$

which is expected to be valid for dilute suspensions at large S and t. In particular, a value close to one is found for z in the DLCA limit [31]. Statistical errors for $n_m(t)$ are very large in our data but quantity $N_m(t)=\sum_{l=1}^{m} n_l(t)$ is a fairly smooth function of m. It follows straightforwardly from Eq. (2) that $N_m(t)$ scales as

$$N_m(t) \sim m^{-1} g(m/t^z) , \tag{3}$$

where $g(x)$ depends on cluster mobility and the dimension. The product $mN_m(t)$ [$N_m(t)$ is normalized to a unit surface] is plotted versus m/t^z (with $z=1.0$) for two different electrolyte concentrations in Fig. 7. The data points correspond to various values of t for the dilute latex dispersion. It is remarkable that all the data for $1M$ NaCl solution collapse on a single universal curve which covers over three orders of magnitude in m/t. For $0.25M$ NaCl solution the data collapse onto a single curve only for $m/t > 1$. Thus the scaling rule given by

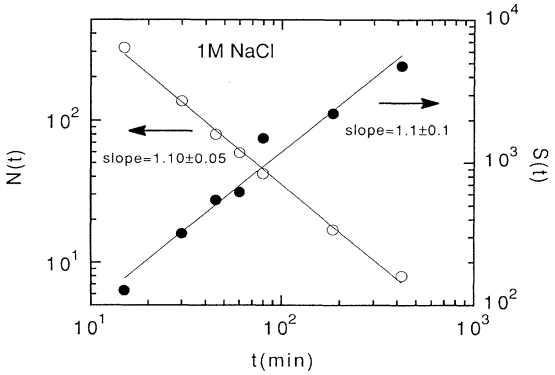

FIG. 6. Total number of clusters $N(t)$ and mean cluster size $S(t)$ as a function of aggregation time for a dilute latex dispersion on a $1M$ NaCl solution.

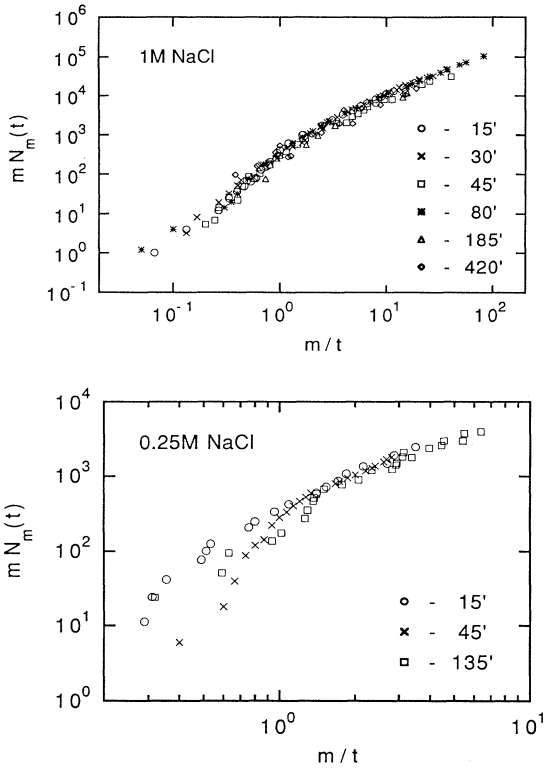

FIG. 7. Scaling of the time-dependent cluster-size distributions for a dilute latex dispersion for two different electrolyte concentrations.

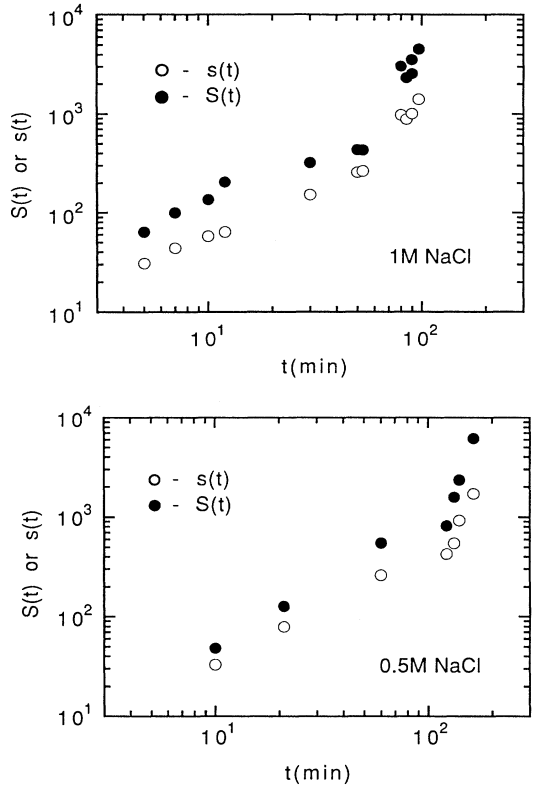

FIG. 9. Number, $s(t)$, and mass, $S(t)$, average aggregate size as a function of time for more concentrated latex dispersion at two different electrolyte solutions.

Eq. (2) is consistent with our experimental results for dilute latex concentrations.

Figure 8 illustrates how the cluster mass distribution varies with cluster mass for two different aggregation times. A well-defined peak is observed in $n_m(t)$; for small masses, $n_m(t)$ is very small. A cluster-size-dependent diffusion coefficient would produce this effect, as numerical simulations have shown [31]. In addition, a mass-dependent sticking probability may have a similar effect on $n_m(t)$ [29].

The kinetics of cluster-cluster aggregation at higher polystyrene-particle concentration is more complex. Figure 9 shows how $S(t)$ and $s(t)=\sum_m m n_m(t)/\sum_m n_m(t)$ depend on aggregation time for two different electrolyte concentrations. A nonlinear behavior is evident for large t. Both $S(t)$ and $s(t)$ increase about linearly with time for $t<100$ min but grow faster at larger times. In the latter region, $z>2$ if the relation $S(t)\sim t^z$ is assumed. We are not in a position to make any statement about this behavior because of large errors in our data and small range of time studied.

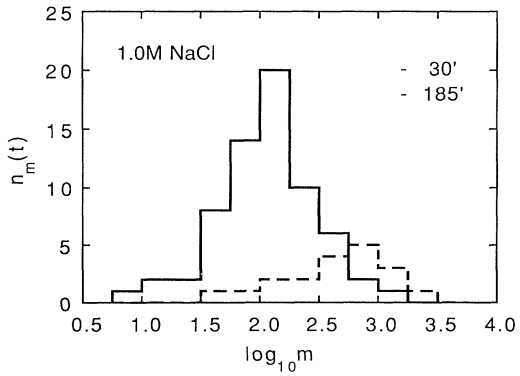

FIG. 8. Cluster-size distribution for two different aggregation times for a 1M NaCl solution and a dilute latex dispersion.

IV. CONCLUSIONS

The fractal dimension of aggregates and the dynamic cluster-size distribution were obtained at various stages of (salt-induced) latex aggregation in two dimensions. We find that the fractal dimension increases as aggregation proceeds. (Anisotropic repulsive interactions favoring aggregation on tips may account for the low values of D observed for short times, while restructuring of clusters can give rise to D increasing with time). The fractal dimension is insensitive to electrolyte concentration; however, electrolyte concentration controls the aggregation rate. Our results for the kinetics of aggregation are in good agreement with recent scaling theory [2]. The bell-shaped cluster distributions obtained suggest that cluster-size-dependent mobility is important in aggregation. The estimated value (1) of the scaling exponent z

shows that our experiments are in fast (DLCA) or quasi-fast aggregation regime. Deviations from this behavior are observed at larger latex concentrations.

ACKNOWLEDGMENTS

We are indebted to Dr. J. F. Fernández for valuable discussions, constant encouragement, and comments on the manuscript. All polystyrene latex used was kindly provided by D. Bastos González and Dr. F. J. de las Nieves. We wish to express our gratitude to F. Martínez López for helping us to digitize images; to J. Díaz for letting us use his optical equipment, and to Dr. J. Marro for letting us use his computer facilities. This work was supported in part by the Comisión Interministerial de Ciencia y Tecnología (Spain), Project No. MAT90-0695-C02-01. One of us (J.S.) likes to thank Departamento de Física Aplicada of Universidad de Granada, Junta de Andalucía (Spain), Fundación Gran Mariscal de Ayacucho (Venezuela), and Consejo Nacional de Investigaciones Científicas y Tecnológicas of Venezuela for financial support for a sabbatical stay at Universidad de Granada.

[1] *Kinetic Aggregation and Gelation,* edited by F. Family and D. P. Landau (Elsevier, Amsterdam, 1984).
[2] T. Vicsek and F. Family, Phys. Rev. Lett. **52**, 1669 (1984).
[3] M. Y. Lin, H. M. Lindsay, D. A. Weitz, R. C. Ball, R. Klein, and P. Meakin, Phys. Rev. Lett. **54**, 1416 (1985).
[4] M. Y. Lin, H. M. Lindsay, D. A. Weitz, R. C. Ball, R. Klein, and P. Meakin, Proc. R. Soc. London, Ser. A **423**, 71 (1989).
[5] M. Y. Lin, H. M. Lindsay, D. A. Weitz, R. C. Ball, R. Klein, and P. Meakin, Phys. Rev. A **41**, 2005 (1990).
[6] P. Meakin, Phys. Rev. A **38**, 4799 (1988).
[7] P. Meakin, Phys. Rev. Lett. **51**, 1119 (1983).
[8] D. H. Sutherland, J. Colloid Interface Sci. **25**, 373 (1967).
[9] G. K. von Schulthess and G. B. Benedek, Macromolecules **13**, 939 (1980).
[10] B. B. Mandelbrot, *The Fractal Geometry of Nature* (Freeman, San Francisco, 1982).
[11] D. A. Weitz, J. S. Huang, M. Y. Lin, and J. Sung, Phys. Rev. Lett. **54**, 1416 (1985).
[12] M. Carpineti, F. Ferri, M. Giglio, E. Paganini, and U. Perini, Phys. Rev. A **42**, 7347 (1990).
[13] Z. Zhou and B. Chu, Physica A **177**, 93 (1991).
[14] P. Richetti, J. Prost, and P. Burois, J. Phys. Lett. **45**, 1137 (1984).
[15] T. Skjeltorp, Phys. Rev. Lett. **58**, 1444 (1987).
[16] A. J. Hurd and D. W. Schaefer, Phys. Rev. Lett. **54**, 1043 (1985).
[17] P. Meakin and M. Muthukumar, J. Chem. Phys. **91**, 3212 (1989).
[18] R. Jullien, Phys. Rev. Lett. **55**, 1697 (1985).
[19] R. Jullien, J. Phys. A **19**, 2129 (1986).
[20] D. Bastos González (unpublished).
[21] J. W. Goodwin, R. H. Ottewill, and A. Parentich, J. Phys. Chem. **84**, 1580 (1980).
[22] J. Lykema, in *Solid/Liquid Dispersions,* edited by Th. F. Tadros (Academic, London, 1987), p. 79.
[23] F. Hausdorff, Math. Ann. **79**, 157 (1919).
[24] P. Pieranski, Phys. Rev. Lett. **45**, 569 (1980).
[25] C. Aubert and D. S. Cannell, Phys. Rev. Lett. **56**, 738 (1986).
[26] W. Y. Shih, I. A. Aksay, and R. Kikuchi, Phys. Rev. A **36**, 5015 (1987).
[27] P. Dimon, S. K. Sinha, D. A. Weitz, C. R. Safinya, G. S. Smith, W. A. Varady, and H. M. Lindsay, Phys. Rev. Lett. **57**, 595 (1986).
[28] J. E. Martin, J. P. Wilcoxon, D. Schaefer, and J. Odinek, Phys. Rev. A **41**, 4379 (1990).
[29] F. Family, P. Meakin, and T. Vicsek, J. Chem. Phys. **83**, 4144 (1985).
[30] M. Kolb, Phys. Rev. Lett. **53**, 1653 (1984).
[31] P. Meakin, T. Viscek, and F. Family, Phys. Rev. B **31**, 564 (1985).
[32] R. Bolet and R. Jullien, J. Phys. A **17**, 2517 (1984).

(a)

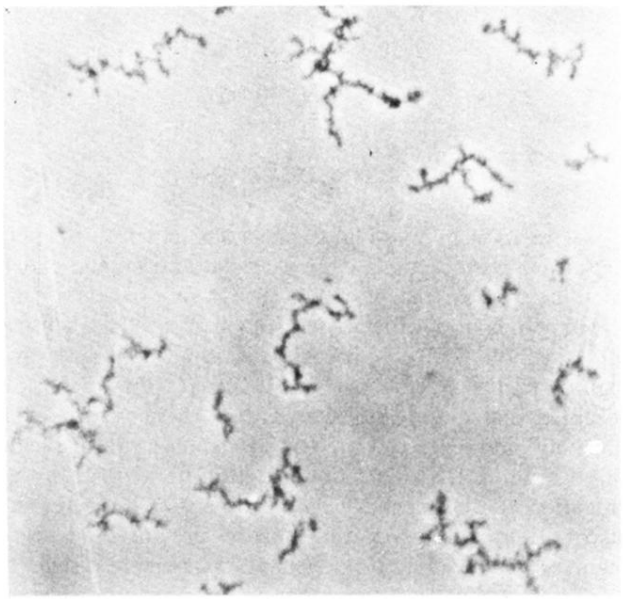

(b)

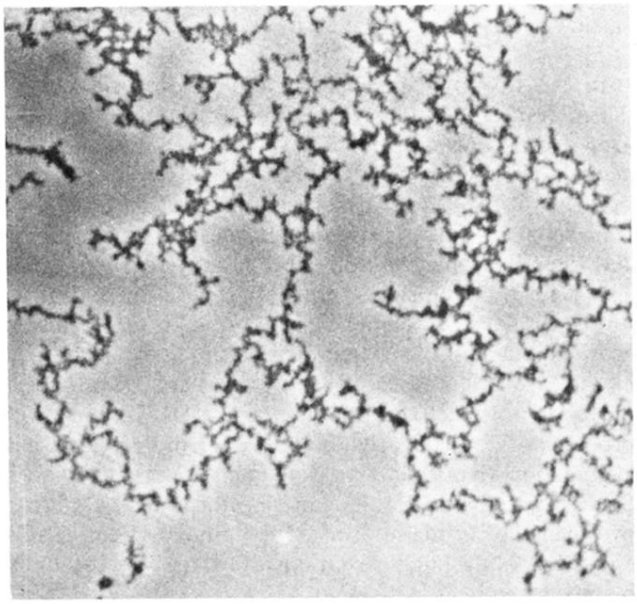

FIG. 1. Photograph of clusters obtained for 1.5M NaCl at two aggregation stages: (a) 10 min and (b) 270 min after dispersion. Area shown is about 150×150 μm^2.